Synthesis and Characterization of Branched Mesogen-Jacketed Liquid Crystal Polymers Based on 2,5-Bis[(4′-methoxyphenyl)oxycarbonyl]styrene and 4-Chloromethylstyrene

Xue Mei, Anhua Liu, Jiaxi Cui, Xinhua Wan,* and Qifeng Zhou*

Beijing National Laboratory for Molecular Sciences, Key Laboratory of Polymer Chemistry and Physics of MOE, College of Chemistry and Molecular Engineering, Peking University, Beijing 100871, China

Received November 6, 2007; Revised Manuscript Received December 19, 2007

ABSTRACT: A series of branched mesogen-jacketed liquid crystal polymers were synthesized via atom transfer radical copolymerization of mesogenic 2,5-bis[(4′-methoxyphenyl)oxycarbonyl]styrene (MPCS) and nonmesogenic 4-chloromethylstyrene (CMS) catalyzed by the $CuCl/CuCl_2$/bipyridine complex in anisole solution at 110 °C. During the early period of polymerization, CMS acted mainly as an initiator to induce the polymerization of MPCS. The molecular weights (MWs) of the resultant polymers increased linearly with monomer conversion and showed a symmetrical and relatively narrow distribution. With the proceeding of polymerization, MWs changed from monomodal to multimodal distribution, indicating the formation of branched structure through the action of vinyl group of CMS. This mechanism was also supported by the increased chain density estimated by a combination of gel permeation chromatography and laser light scattering, end-group analysis, and the reactivity ratios of two monomers ($r_{MPCS} = 0.71$, $r_{CMS} = 0.10$). The thermotropic properties of the copolymers strongly relied on the feed ratio of MPCS to CMS and MW. The feed ratio of MPCS to CMS should be at least 30 with high enough MW. For the copolymer obtained at the feed ratio of 32, the minimum $M_{n,GPC}$ was 1.21×10^4 Da to achieve a mesophase. Although linear poly{2,5-bis[(4′-methoxyphenyl)oxycarbonyl]styrene} displayed columnar nematic phase (Φ_N) and hexatic columnar nematic phase (Φ_{HN}) depending on MW, the branched polymer showed just a Φ_N phase, indicating the remarkable depressing effect of the branched structure on the mesomorphic property.

Introduction

Dendrimers and hyperbranched polymers have gained broad interests for their highly functionalized, three-dimensional fractal structures with respect to their linear counterparts and for their promising potential applications in process additives, coatings, catalysts, sensors, and nanotemplates.[1−4] However, such polymers disfavor the formation of mesophase because the mesogens on the treelike skeleton are not prone to pack orderedly. In 1992, Kim reported the synthesis of hyperbranched aromatic polyamides with lytropic properties although the mechanism of mesophase formation remains unclear until now.[5] Percec and co-workers for the first time reported the synthesis of thermotropic hyperbranched polyethers with hexagonal columnar phase (Φ_H) and nematic phases.[6−9] In both cases, either disklike mesogens (the former) or rodlike mesogens (the later) are incorporated into the polymer framework as in main-chain liquid crystalline polymers (MC-LCPs). The key for these polymers to generate mesophases is the utilization of flexible spacers between mesogens, which enables the mesogens to undergo conformational change from treelike form into the compact, geometrically anisotropic form. In other words, hyperbranched polymers with totally rigid units are not ready to form thermotropic mesophase.

Jin et al. studied systematically the liquid crystalline (LC) properties of hyperbranched polyesters.[10,11] In the system that branches emanated from the central part of mesogens, the polymers formed nematic phase only when the terminals groups were carboxylic acids. Esterification of carboxylic terminals diminished LC property completely.[10] The formation of mesophase was attributed to the intermolecular hydrogen bonds between carboxylic acids, which caused the macromolecules to take rodlike shape. However, when the branches were linked to flexible spacers, nematic phase was obtained no matter the terminals were acids or esters.[11] They thought the increased conformational freedom of the polymers built up in this way made the mesogens easier to orient parallelly. Biodegradable hyperbranched LC polyesters and chiral hyperbranced LC polyesters have also been reported by Kricheldorf,[12,13] Ringsdorf,[14] and their co-workers.

Among all these polymers, mesogen is a part of each branching monomer. Mesogen can also be coupled to the end groups of the scaffold. Frey and co-workers synthesized mesogen-terminated hyperbranched polyglycerols based on 2,3-epoxy-1-propanol.[15] Unlike the dendrimers with mesogenic end groups,[16] which prefer to form smectic phase, polyglycerol formed nematic phase since the mesogens were located at different distances from the core. It is interesting that attaching mesogens to scaffolds through ionic interaction plays the same role to generate mesophase.[16] Xi,[17] Yan,[18] and their co-workers employed a different approach to prepared hyperbranched LCPs with similar architecture. In their systems, the peripheries of flexible scaffolds did not contain attached mesogens but were grafted from SC-LCPs. Other interesting examples include LC polysiloxanes.[19]

Most of the thermotropic LC hyperbranched polymers reported up to now, especially for those with mesogen as a part of scaffold, were obtained by step-growth polymerization. In a rapid communication, He and Yan reported the synthesis of a series of branched side-chain LCPs (SC-LCPs) based on 2-(2-bromoisobutyryloxy)ethyl methacrylate (inimer) and 6-(4-methoxy-azobenzene-4′-oxy)hexyl methacrylate (comonomer) through

* To whom correspondence should be addressed: Ph 86-10-6275 4187, Fax 86-10-6275 1708, e-mail xhwan@pku.edu.cn, qfzhou@pku.edu.cn.

10.1021/ma7024368 CCC: $40.75
Published on Web 01/30/2008

atom transfer radical self-condensing vinyl copolymerization (ATR-SCVCP),[20] which was first developed by Fréchet et al.[21,22] In these polymers, the mesogenic units were appended to polymer framework at the end via flexible spacers. Thereafter, their ordered arrangements in melt were expected to be less influenced by the branching points than in above-mentioned hyperbranched LCPs, where the mesogenic units were incorporated into polymer skeleton at the two ends. It was found that both smectic and nematic phases were observed in a copolymer only when the feed molar ratio of comonomer to inimer was greater than 8.

Mesogen-jacketed liquid crystal polymers (MJLCPs) stand for an unique type of SC-LCPs with the mesogens laterally attached to flexible polymer backbone on each repeating unit via no or only short spacers.[23,24] The high crowding of bulky and rigid side groups forces the polymer main chain to adopt an extended conformation as in semirigid or rigid MC-LCPs. As a result, although MJLCPs belong to SC-LCPs chemically, they display many thermotropic properties characterized by MC-LCPs, such as high glass transition temperature,[25] broad temperature range of mesophase,[26] long persistence length in good solvent,[27,28] and forming banded texture after mechanical shearing in LC state.[29,30] Even more interesting is that it can be produced by chain polymerization and allow for control over macromolecular architecture using living radical polymerization techniques.[31] Poly{2,5-bis[(4′-methoxyphenyl)oxycarbonyl]styrene} (PMPCS) is one of the most intensively studied MJLCPs.[32] Its LC property is strongly dependent on molecular weight (MW).[33] When number-average molecular (M_n) is less than 8×10^3 Da, no mesophase is generated; when M_n is larger than 8×10^3 Da but less than 1.6×10^4 Da, columnar nematic phase (Φ_N) is generated; when M_n is higher than 1.6×10^4 Da, hexatic columnar nematic phase (Φ_{HN}) is achieved. The polymer has also been employed as building blocks to construct rod−coil di- and triblock copolymers, which display beautiful and well-controlled supramolecular structures in both solution and bulk and show interesting properties.[34−37] Recently, Pan et al. reported synthesis and characterization of a series of eight-arm star PMPCS obtained by atom transfer radical polymerization initiated by octakis(2-bromo-2-methylpropionoxypropyldimethylsiloxy)octasilsesquioxane.[38] It was found that the starlike architecture remarkably influenced the mesomorphic properties of the polymers. The length of each arm for the polymer to generate mesophase is shorter in eight-arm star PMPCS than in linear ones.

Herein, we will report on the synthesis and LC properties of branched PMPCSs by ATR-SCVCP of a nonmesogenic inimer, 4-chloromethylstyrene (CMS), with a mesogenic comonomer, 2,5-bis[(4′-methoxyphenyl)oxycarbonyl]styrene (MPCS). In the copolymers, PMPCS chains in between the two branching points constitute LC segments, while CMS provides branched structures. The control over the degree of branching (DB) and length of PMPCS segment are achieved by varying the feed ratio of MPCS to CMS. The overall MW was adjusted by reaction time. The thermotropic properties are explored by combinatory techniques of differential scanning calorimetry, polarized light optical microscopy, and wide-angle X-ray diffractometry. Thus, constructed macromolecules distinguish other hyperbranched LC polymers with built-in mesogens by two facts. First, they are synthesized by radical polymerization, which can be carried out under relatively undemanding conditions and does not require ultrapure solvent and reagent. Second, the overall MW and the length of LC segment between branching points can be tailored separately, which allows for a comprehensive investigation of the branched structure effect on the mesomorphic properties of the resultant polymers.

Experimental Section

Materials. The monomer MPCS was synthesized according to the procedure reported previously.[32] CMS (Acros, 90%) was purified by passing through a neutral Al_2O_3 column to remove inhibitor. Anisole (Beijing Chemical Co., A.R.) was refluxed over calcium hydride (Beijing Chemical Co., A.R.) and distilled out just before use under an argon atmosphere. CuCl was washed with hydrochloric acid (Beijing Chemical Co., 36%), deionized water, and acetic acid (Beijing Chemical Co., A.R.) and dried at 60 °C under vacuum for 12 h. Bipyridine (Bipy, Beijing Chemical Co., A.R.) was purified by recrystallization from ethanol. Dicumyl peroxide (DCP, Akzo Nobel, 98%) was purified by recrystallization from methanol. Tetrahydrofuran (THF, Aldrich, gas chromatography grade) was directly used in the gel permeation chromatography (GPC) and laser light scattering measurements. Other solvents and reagents were purchased from Beijing Chemical Co. and used as received unless otherwise specified.

Atom Transfer Radical Copolymerization. The atom transform radical copolymerization of MPCS and CMS was carried out in solution. A typical reaction procedure was described as follows: MPCS (0.2 g, 0.50 mmol), CMS (0.0024 g, 0.015 mmol), CuCl (0.0015 g, 0.015 mmol), $CuCl_2$ (0.0002 g, 0.0015 mmol), bipy (0.0072 g, 0.046 mmol), and anisole (0.3 g) were successively introduced into a reaction tube. After three freeze−pump−thaw cycles, the tube was sealed under vacuum and inserted into a thermostated oil bath at 110 °C. The reaction was allowed to continue for 4 h. After breaking the tube to terminate the polymerization, the reaction mixture was diluted with 20 mL of THF and let to pass through a short Al_2O_3 column to separate the catalyst and then precipitated in 250 mL of methanol. The precipitate was collected by filtration and washed with methanol three times and dried at 40 °C under vacuum for 24 h before further characterization. The monomer conversion in weight was 68.2%. The number-average molecular weight and polydispersity of the resultant copolymer detected by GPC were 7.6×10^3 Da and 1.50, respectively. ^{1}H NMR (δ, ppm, acetone-d_6): 1.2−2.0 (broad peaks, $-CH_2CH$ protons in the backbone), 3.2−3.7 (broad peaks, $-OCH_3$ protons in MPCS), 5.1−5.2 and 5.5−5.7 (broad peaks, vinyl protons of polymers), 5.3−5.4 (tripartite peaks, −CHCl protons of MPCS ends), 6.2−7.0 (broad peaks, protons of the side phenyl ring of MPCS and aromatic protons of CMS), and 7.1−7.9 (broad peaks, protons of the middle phenyl ring of MPCS).

Instruments and Measurements. The number-average molecular weight ($M_{n,GPC}$), weight-average molecular weight ($M_{w,GPC}$), and polydispersity distribution index ($PDI_{GPC} = M_{w,GPC}/M_{n,GPC}$) of the resultant copolymers were estimated on a gel permeation chromatograph (GPC) equipped with a Waters 515 HPLC pump and a Waters 2410 refractive index detector. Three Waters Styragel columns with 10 μm size bead were connected in tandem. Their effective molecular weight ranges were 100−10 000 for Styragel HT2, 500−30 000 for Styragel HT3, and 5000−600 000 for Styragel HT4. The pore sizes were 50, 100, and 1000 nm for Styragels HT2, HT3, and HT4, respectively. THF was used as the eluent at a flow rate of 1.0 mL/min at 35 °C. The calibrating curve was obtained against a series of polystyrene standards.

The number-average molecular weight ($M_{n,GPC-LS}$), weight-average molecular weight ($M_{w,GPC-LS}$), and polydispersity distribution index ($PDI_{GPC-LS} = M_{w,GPC-LS}/M_{n,GPC-LS}$) of the resultant copolymers were also characterized by a GPC−light scattering online technique. A Wyatt Technology DAWN HELEOS 18 angle (from 15° to 165°) light scattering detector with a Ga−As laser (658 nm, 40 mW) was connected to the same GPC instrument mentioned above to replace the Waters 2410 refractive index detector. The concentration at each elution volume was determined with a Wyatt Optilab Rex interferometeric differential refractometer (658 nm). The molecular weight data were calculated using Astra 5.1.6.0 software (Wyatt Technology). The refractive index incre-

Table 1. Polymerization Results and Properties of the Branched Polymers Obtained at a Feed Molar Ratio of MPCS to CMS of 32

run[a]	time (h)	conv (%)	$M_{n,GPC}$[b] ($\times 10^{-4}$)	PDI_{GPC}[b]	$M_{n,GPC-LS}$[c] ($\times 10^{-4}$)	PDI_{GPC-LS}[c]	T_g[d] (°C)	liquid crystallinity
BP-1	0.5	1.1	0.23	1.09				no
BP-2	1	12.2	0.31	1.23	1.09	1.18	122	no
BP-3	2	17.5	0.33	1.27	1.23	1.18	122	no
BP-4	3	36.8	0.44	1.32	1.96	1.12	113	no
BP-5	4	68.2	0.76	1.50	2.49	1.18	128	no
BP-6	8	94.5	1.21	1.74	3.79	1.45	130	yes
BP-7	16	95.6	2.61	2.33	8.39	2.68	132	yes
BP-8	24	92.5	3.47	2.63	14.34	2.54	132	yes
BP-9	48	87.9[e]	4.57	2.90	46.82	1.87	132	yes

[a] Polymerization conditions: anisole solution (40 wt %); temperature, 110 ± 0.5 °C; [CMS]/[CuCl]/[$CuCl_2$]/[Bipy] = 1:1:0.1:3. [b] Number-average molecular weight ($M_{n,GPC}$), weight-average molecular werght ($M_{w,GPC}$), and polydispersity index ($PDI_{GPC} = M_{w,GPC}/M_{n,GPC}$) were obtained by gel permeation chromatography, calibrated against a series of polystyrene standards. [c] Nmber-average molecular weight ($M_{n,GPC-LS}$), weight-average molecular weight ($M_{w,GPC-LS}$), and polydispersity index ($PDI_{GPC-LS} = M_{w,GPC-LS}/M_{n,GPC-LS}$) were estimated at 35 °C with a GPC−light scattering online technique. [d] Glass transition temperature was obtained from the second heating differential scanning calorimetry themogram. [e] Some insoluble matters were formed.

ment (d*n*/d*c*) of BP-5 was estimated as 0.179 mL/g in THF at room temperature by an Optilab Rex interferometeric refractometer (Wyatt Technology) at the wavelength of 658 nm. The sample concentrations were 1.0, 2.0, 3.0, 4.0, and 5.0 mg/mL. The refractometer was calibrated with aqueous NaCl solution. All samples were dissolved in THF and stayed overnight before filtration through a 0.45 μm PTFE filter.

The thermal transitions of the copolymers were detected using differential scanning calorimetry (DSC) on a TA Q100 calorimeter in a temperature range from 0 to 200 °C at a heating rate of 20 °C min^{-1} under a continuous nitrogen flow. All the data were collected during the second heating process after cooling at 5 °C min^{-1} from 200 °C. *n*-Octane (mp 56.8 °C) and indium (mp 156.8 °C) were used to calibrate the instrument. The average sample mass was about 4 mg, and the nitrogen flow rate was 50 mL min^{-1}. Thermogravimetric analysis (TGA) was performed on a TA Q600 instrument at a heating rate of 10 °C/min under a nitrogen atmosphere.

Polarized optical microscopy (POM) was conducted on a Leica DML polarized light optical microscope coupled with a Linkam TH-600PM hot stage. The sample films with thicknesses of several microns were prepared by the solution-cast method.

One-dimensional wide-angle X-ray diffraction (1D-WAXD) powder experiments were run on a Philips X'Pert Pro diffractometer with a 3 kW ceramic tube as the X-ray source (Cu Kα) and an X'celerator detector. To approach the structure evolution as a function of temperature, a temperature control unit was connected to diffractometer. Background scattering was recorded and subtracted from the samples patterns.

Two-dimensional wide-angle X-ray diffraction (2D-WAXD) fiber patterns were recorded on a Bruker D8 Discover diffractometer with GADDS (general area detector diffraction system) as a 2D detector. Fibers were drawn at a rate of about 1 m s^{-1} at 240 °C and quenched to room temperature. The point-focused X-ray beam was aligned either perpendicular or parallel to the mechanical shearing direction of the samples mounted on the samples stage. The 2D diffraction patterns were obtained in a transmission mode at room temperature. Background scattering was recorded and subtracted from the samples patterns.

Results and Discussion

ATR−SCVCP. Branched MJLCPs based on MPCS and CMS were obtained via ATR−SCVCP, which was carried out in anisole at 110 °C using CuCl/$CuCl_2$/bipy complex as the catalyst. Nonmesogenic CMS acted as an inimer, while mesogenic MPCS as a comonomer. $CuCl_2$ was employed to reduce the concentration of propagating radicals during copolymerization.[39] The feed molar ratio of MPCS to CMS and reaction time were varied to adjust DBs and overall MWs of the resultant copolymers. The size of the copolymers was estimated by both GPC and GPC-LS online techniques.

Table 1 depicts the polymerization results and the properties of the copolymers obtained at a constant [MPCS]/[CMS] value of 32. The copolymerization proceeded at a quite rapid rate. As shown in Table 1, the monomer conversion in total reached 94.5% in 8 h. Extending reaction time beyond 16 h led to an apparent decrease in monomer conversion because a certain amount of gels formed and were separated after reaction, which reduced the weights of the copolymers obtained. The insoluble gels might be formed by the intermolecular cross-linking of propagation radicals due to much lower concentration of MPCS during the late stage of polymerization. Figure 1 shows the GPC traces of the copolymers obtained at different reaction time. When the reaction time was less than 4 h, all the curves were symmetrical and relatively narrow, indicating a well-controlled polymerization process.[31,33] When the reaction time was equal to or higher than 4 h, the GPC patterns changed from monomodal, narrow distribution to multimodal, broad distribution. It meant the formation of branched structures.[40]

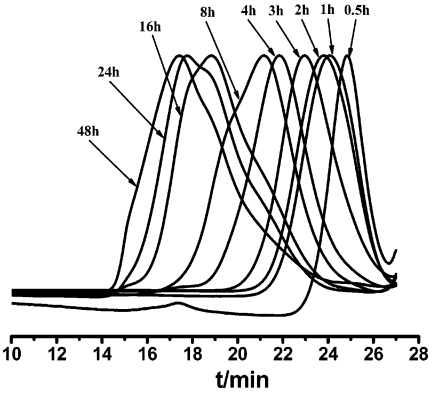

Figure 1. GPC curves of the branched polymers based on CMS and MPCS obtained at different reaction time. The polymerization conditions were the same with that of Table 1.

The speculation on the formation of branched structures was also supported by the discrepancy between $M_{w,GPC}$ and $M_{w,GPC-LS}$. It was evident from Table 1 that MWs determined by GPC-LS were much higher than those deduced by GPC, and the difference became larger with the proceeding of polymerization. Especially, at the reaction time of 48 h, $M_{w,GPC-LS}$ was about 7 times larger than $M_{w,GPC}$. The deviation at early stage of polymerization was probably caused by the fact that the hydrodynamic volumes of the copolymers obtained differed substantially from those of polystyrene standards, whereas the increased discrepancy with reaction time was probably due to the densification of the chains with the formation of branched structures.

End-Group Analysis. Hyperbranched polymers produced from CMS are characterized by one double bond head group and many chloromethyl and chloromethine end groups. The

Table 2. Polymerization Results and Properties of the Branched Polymers Obtained at a Feed Molar Ratio of MPCS to CMS of 10 under Otherwise the Same Reaction Condition with That of Table 1

run	time (h)	conv (%)	$M_{n,GPC}$ ($\times 10^{-4}$)	PDI_{GPC}	$M_{n,GPC-LS}$ ($\times 10^{-4}$)	PDI_{GPC-LS}	T_g (°C)
BP-10	1/3	20.3					113
BP-11	2/3	36.3	0.23	1.30			114
BP-12	1	57.7	0.29	1.30	1.24	1.18	121
BP-13	2	87.6	0.46	1.55	1.73	1.30	134
BP-14	4	95.9	0.81	2.22	2.86	1.75	131
BP-15	8	95.9	1.58	3.99	9.33	2.45	132

number of end groups equals the degree of polymerization (DP)[40] if side-reactions like chain transfer and termination are ignored. To analyze the end-group structure of branched PMPCS, a series of copolymers were prepared under identical conditions of Table 1, except for a different MPCS to CMS feed molar ratio of 10. The GPC curves of the copolymers obtained at different reaction time had a changing tendency with reaction time similar to that shown in Figure 1, i.e., from monomodal distribution to multimodal distribution (Figure S1). However, the critical reaction time at which the transition took place was quite different. At [MPCS]/[CMS] = 32, the critical time was around 4 h, while that at [MPCS]/[CMS] = 10 was 1 h. The difference implied that more CMS in feed favored the formation of the branched structures. The polymerization results are summarized in Table 2. The difference between $M_{w,\,GPC}$ and $M_{w,\,GPC-LS}$ also increased with reaction time.

Figure 2 exhibits the ^{1}H NMR spectra of the branched polymers obtained at different reaction time with a fixed [MPCS]/[CMS] value of 10. The inset displays the enlarged curves in the chemical shift range from 4.8 to 5.9 ppm. The two broad resonance bands centered at 5.2 and 5.7 ppm were assigned to cis and trans β-vinylic protons of head groups derived from CMS, while the triplet peaks at 5.3 ppm were due to secondary benzylic chloride protons. No signal of chloromethyl group was observed. It might imply that all CMS took part in the initiation of MPCS almost simultaneously and were consumed completely soon after polymerization began. This was consistent with the conclusion from GPC and light scattering studies. Unfortunately, we could not calculate the numbers of branched points in each polymer with these data due to the weak intensity of the secondary benzylic chloride proton of MPCS relative to the real contents, which might result from the low mobility of rigid polymer main chains.[41] Extending reaction time led to a remarkable increase in the area ratio of end secondary benzylic protons to head β-vinylic protons.

Radical copolymerization of MPCS with CMS was carried out in anisole at 110 °C employing DCP as the initiator (see Supporting Information). The reactivity ratios of MPCS (r_{MPCS}) and CMS (r_{CMS}) were estimated as 0.71 and 0.10, respectively, with the Kelen−Tudos (K−T) linearization method[42] based on the feed monomer ratios (0.1−0.90) and the copolymer compositions characterized by ^{1}H NMR spectroscopy (Figure S2 and Table S1). The fact of $r_{MPCS} > r_{CMS}$ implied that MPCS was more reactive than CMS in radical copolymerization. This was consistent with the copolymerization of St with MPCS. When MPCS copolymerized with St, MPCS showed much higher reactivity ($r_{MPCS} = 4.15$) than St ($r_{St} = 0.44$), which was attributed to the electron-withdrawing effect of ester groups and conjugate effect.[43] Ober and co-workers noticed the similar behavior in nitroxide-mediated free radical polymerization of 2,5-bis[(4′-butylbenzoyl)oxy]styrene (BBOS).[44] In bulk, BBOS polymerized much faster than its nonmesogenic, electron-deficient model, 2,5-diacetoxystyrene, whereas in a dilute solution, the polymerization rates of both monomers were comparable. The increased reactivity of BBOS in bulk was attributed to the presence of a nematic phase which led to localized ordering of the monomers. It should be noted that the reaction temperature was at 110 °C. It is reasonable to think that chain transfer to CMS took place to an appreciable extent. As a result, the reactivity ratios evaluated in this way should differ from the real values.

ATR−SCVCP Mechanism. On the basis of the above results, a tentative copolymerization mechanism of MPCS and CMS was proposed as shown in Scheme 1. At the beginning of polymerization, CMS acted mainly as an initiator to induce atom transfer radical polymerization (ATRP) of MPCS under the catalysis of $CuCl/CuCl_2$/bipy due to its relatively low concentration and reactivity with respect to MPCS. The resultant polymers were actually linear PMPCS terminated by 4-vinylphenylmethyl and chloromethine at two ends, respectively. Extending reaction time decreased the concentration of MPCS and enabled more linear PMPCS with 4-vinylphenylmethyl head to react with itself through the action of head vinyl group in addition to with MPCS, leading to the formation of branched intermediates with different size and multiinitiating sites. When all the monomers were consumed, the branched polymers would solely react with themselves, and the macromolecules would become denser and denser. The MWs estimated by LS would become higher and higher than those estimated by GPC as demonstrated in Tables 1 and 2.

Thermal Behavior. DSC. The thermal transition temperatures of the resultant branched MJLCPs were evaluated by DSC. Since fast heating of slowly cooled samples induces endothermic hysteresis peaks in glass transition region, which makes glass transition more evident, a fast heating rate of 20 °C min^{-1} was employed to scan the annealed copolymers, which were prepared by being slowly cooled (5 °C min^{-1}) from 200 °C to room temperature. The thermograms of all the copolymers were featureless except for glass transitions (Figure S3). The glass transition temperatures (T_gs) of all the copolymers are summarized in Tables 1 and 2. It seemed that T_gs of the copolymers (i.e., BP-1−4) produced at the early stage of ATR−SCVCP were comparable to those of linear PMPCS obtained by conventional radical polymerization or controlled radical polymerization.[32,33] The T_g of linear PMPCS was 119 °C estimated under identical condition. It was another proof that CMS mainly acted as an initiator to induce ATRP of MPCS to give linear PMPCS during the early period of polymerization. When the reaction time exceeded 3 h, the T_gs of the copolymers obtained were about 10 °C higher than their linear counterparts. The similar tendency of T_gs with reaction time can be seen in Table 2.

T_g is a temperature at which the segmental motion of polymer chains caused by the concerted rotation of bonds at the ends of the segment begins. T_g is affected by free volume, structural rigidity, and secondary interaction. Introduction of hyperbranched structures usually decreases T_gs since it provides larger free volume for segment motion and less intermolecular chain entanglement, which increase the mobility of chain segment.[45] However, the T_gs of hyperbranched polymers can also be higher than linear polymers. For example, as reported by Murali and Samui,[46] hyperbranched photoactive benzylidene LC polyesters had higher T_gs than linear ones. It was considered that the cooperative motions of the segments in hyperbranched polymers were impeded by the close interaction between the various segments arranged in the compact architecture. The increased T_g of branched PMPCS with respect to linear PMPCS might be the competition result of several facts. The first fact is

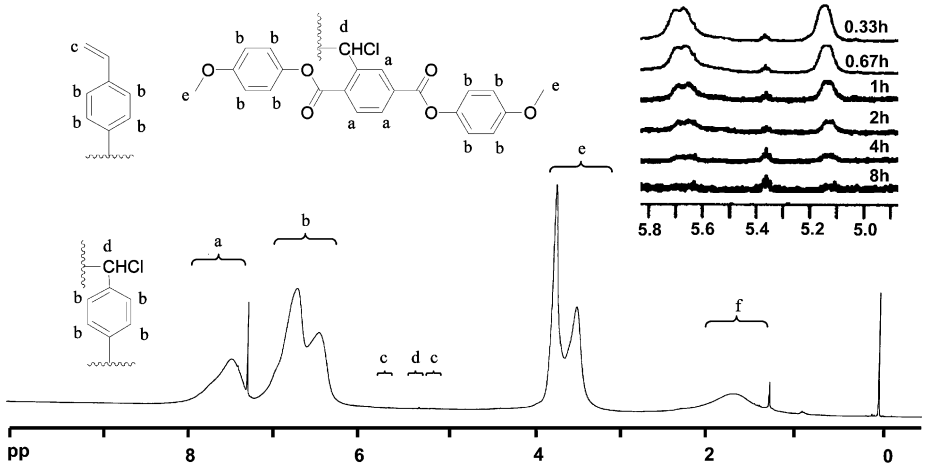

Figure 2. ^{1}H NMR spectra of branched PMPCSs in *d*-chloroform.

Scheme 1. Copolymerization Mechanism of *p*-Chloromethylstyrene (CMS) and 2,5-Bis[(4′-methoxyphenyl)oxycarbonyl]styrene (MPCS)

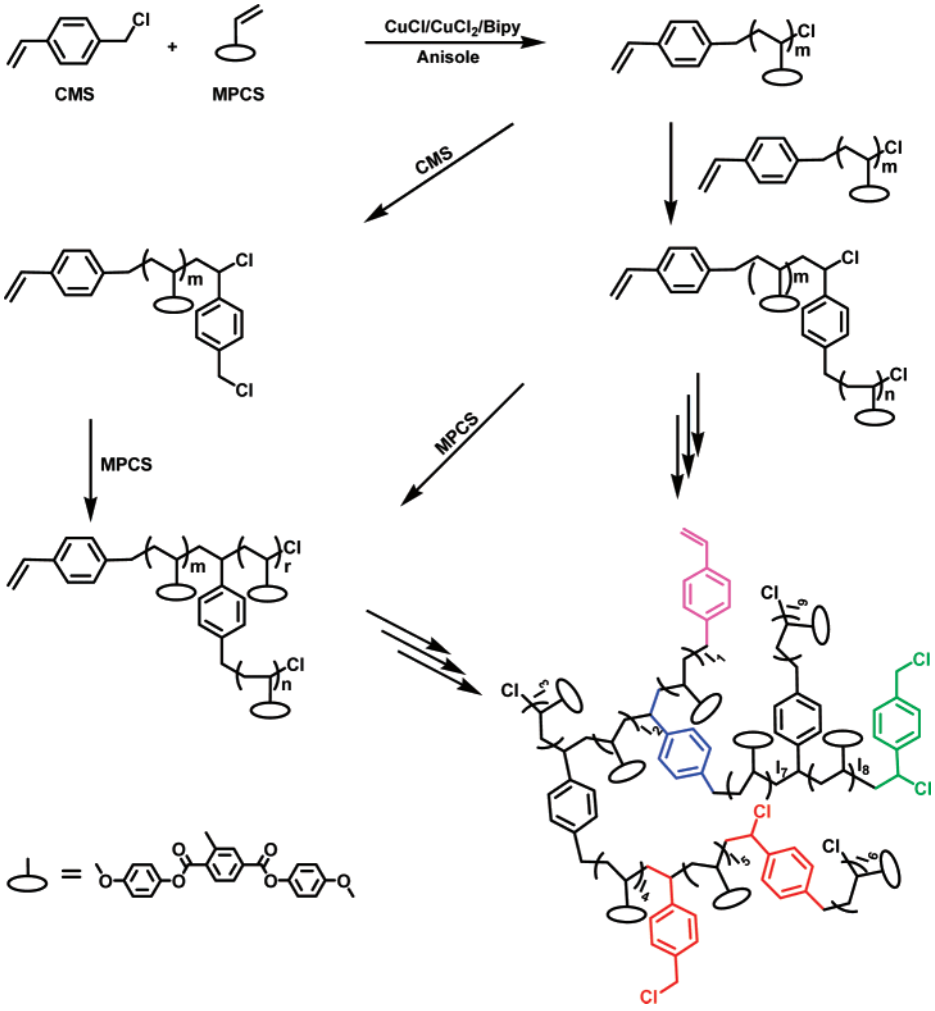

restricted segment motion. In branched PMPCS, CMS formed branching points, while MPCS homopolymer constituted segments between the two branching points. As indicated in the Introduction, although PMPCS is a SC-LCP in terms of its chemical structure, it takes extended conformation and has thermotropic properties of rigid or semirigid MC-LCPs. It is reasonable to think that the long-range chain motion is restricted more significantly in branched PMPCS than in other branched polymers with flexible chains. The second fact is free volume, which include two parts. One is located in the interior of polymer molecules; another is distributed between branched macromolecules. The former is smaller in branched PMPCS than in linear PMPCS as demonstrated by the M_n difference characterized by GPC and GPC-LS on-line technique, respectively. The other was the free volume rooted in the intermolecular interspaces. Since the branched PMPCS had more chain ends which brought further asymmetry, it accumulated in a more incompact mode, producing larger locomotory spaces for the polymer chains.

POM. LC phases of branched PMPCS and random copolymers of CMS and MPCS were first studied by POM. All the branched polymers and random copolymers were white powders at room temperature. Under cross-polarized light, they showed

Table 3. Effect of the Molar Ratio of MPCS to CMS in Feed on the Thermal Properties of the Branched Polymers

run[a]	[MPCS]/[CMS]	$M_{n,GPC}$[b] ($\times 10^{-4}$)	PDI_{GPC}[b]	$M_{n,GPC-LS}$[c] ($\times 10^{-4}$)	PDI_{GPC-LS}[c]	T_g[d] (°C)	liquid crystallinity
PMPCS[e]		2.28	1.44	6.45	1.16	119	yes
BP-16	71/1	2.16	1.43	7.80	1.60	120	yes
BP-17	40/1	3.60	2.37	14.02	2.32	125	yes
BP-18	37/1	3.65	1.99	10.89	2.06	128	yes
BP-8	32/1	3.47	2.63	14.34	2.54	132	yes
BP-19	31/1	3.31	2.77	12.02	2.06	132	yes
BP-20	30/1	2.54	2.77	10.93	2.05	131	yes
BP-21	29/1	1.75	1.96	5.00	1.48	130	no
BP-22	28/1	2.62	2.88	10.25	2.08	132	no
BP-23	27/1	2.50	3.61	28.82	1.92	133	no
BP-24	26/1	2.76	2.86	11.76	2.09	133	no
BP-25	18/1	6.70	1.31	16.68	2.05	133	no

[a] The polymerization condition was the same with that of Table 1.

Table 4. Polymerization Results and Properties of the Branched Polymers Obtained at a Feed Molar Ratio of MPCS to CMS of 28 under Otherwise the Same Reaction Condition as That of Table 1

run[a]	time (h)	conv (%)	$M_{n,GPC}$[b] ($\times 10^{-4}$)	PDI_{GPC}[b]	$M_{n,GPC-LS}$[c] ($\times 10^{-4}$)	PDI_{GPC-LS}[c]	T_g[d] (°C)	liquid crystallinity
BP-22	24	90.5	2.62	2.88	10.25	2.08	132	no
BP-26	48	81.1	4.28	3.15	54.64	1.83	134	no
BP-27	72	81.1	4.00	3.39	108.20	1.38	134	no

only faint birefringence presumably due to the poorly ordered structure formed during precipitation process. Heating the samples to their T_gs, the weak birefringence disappeared immediately. Above T_gs, the thermal behaviors of branched PMPCS depended on the feed molar ratio of MPCS to CMS and the MWs of the resultant copolymers. For the copolymers BP-1−BP-5, no discernible birefringence developed again, indicating the absence of ordered structure in the melt of these samples. For the copolymers BP-7−BP-9, quite strong birefringence appeared almost immediately above their glass transitions and did not vanish on the subsequent heating and cooling processes. It implied that the mesophases formed in these copolymers were very stable. Heating BP-6 to the temperature above its T_g, only weak birefringence formed gradually, suggesting the formation of less ordered mesophase. At 320 °C, the birefringence disappeared completely. Cooling the sample slowly before thermal decomposition, the weak birefringence was observed again. The result suggested the BP-6 could form only less ordered structure and had a reversible order−disorder transition. These results showed the overall MWs of the copolymers had remarkable influence on their thermotropic properties. Since the mesophase structures of linear PMPCS depended on MWs, it is reasonable to think that the length of MPCS segment between branching points should have a minimum value for the branched PMPCS to achieve a mesophase.

According to the polymerization mechanism proposed in the previous section, the length of MPCS segment between branching points was dependent on the feed molar ratio of MPCS to CMS and the general MW of the copolymer was dependent on reaction time. In order to approach the effect of the length of MPCS segment between branching points on the mesomorphic properties of the branched PMPCS, a series of branched copolymers were prepared at a fixed reaction time of 24 h but at varying molar ratios of MPCS to CMS in feed. The polymerization results and the thermotropic properties of the copolymers obtained are depicted in Table 3. All the copolymers had $M_{n,GPC}$ over 5×10^4 Da, which was high enough for a linear PMPCS to possess LC properties. However, only the copolymers obtained at feed MPCS to CMS ratio higher than 29 could form mesophase. This was consistent with our speculation made previously. To investigate MWs dependence of branched PMPCS further, three branched polymers with the feed molar ratio of MPCS to CMS equaled to 28/1 were synthesized. The polymerization results and the properties of the resultant copolymers are summarized in Table 4. Even though all the three copolymers had $M_{n,GPC}$s higher than 2.62×10^4 Da, no mesophase could be generated.

Figure 3 shows the representative images of the textures of BP-16 taken at 180 °C (a) and BP-17 taken at 240 °C (b). Linear

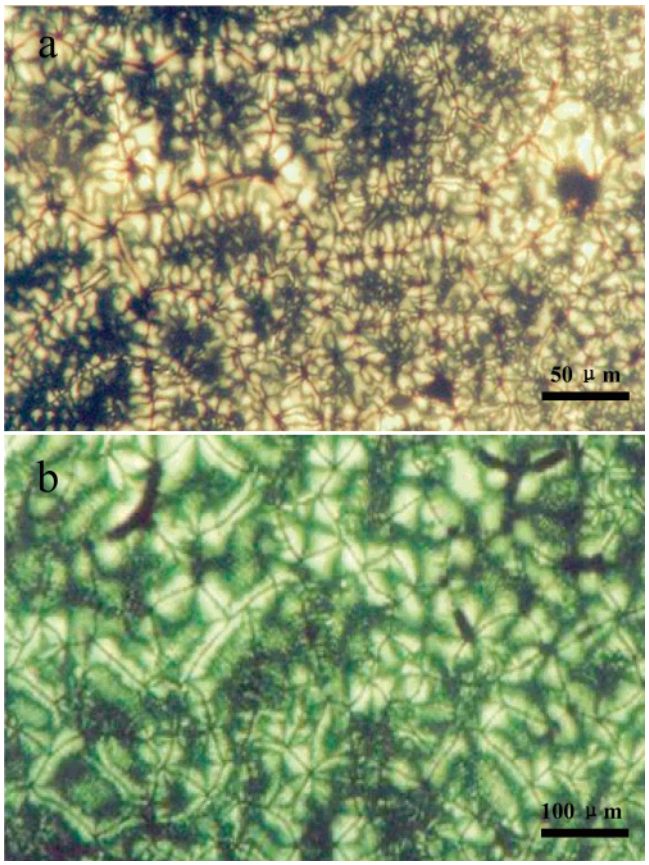

Figure 3. Polarized light optical microphotographs of BP-16 taken at 180 °C (a) and BP-17 taken at 240 °C (b). The polymer films with thickness of about 10 μm were prepared by solution-cast method and annealed at each temperature for 72 h before taking the pictures.

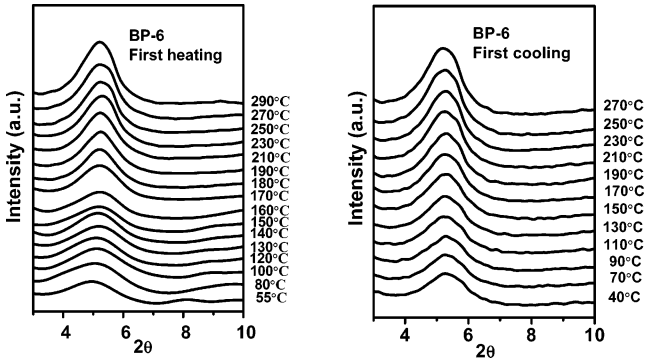

Figure 4. One-dimensional wide-angle X-ray diffraction powder patterns of BP-6 in the low 2θ angle region recorded during the first heating (left) and subsequent cooling course (right).

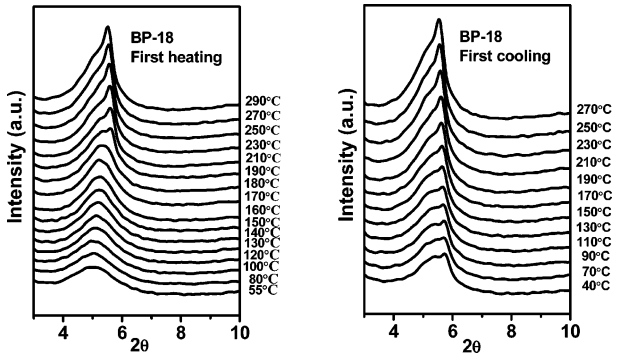

Figure 5. One-dimensional wide-angle X-ray diffraction powder patterns of BP-18 in the low 2θ angle region recorded during the first heating (left) and subsequent cooling course (right).

PMPCS exhibited star-shaped texture with two or four brushes.[33] However, branched PMPCS could only developed schlieren texture. It seemed that the melt viscosity of the branched PMPCS was much higher than that of linear one. The textures of BP-16 and BP-17 were taken after 3 days annealing at the temperatures. Moreover, branched structures restricted significantly the orientation of polymer main chain. Linear PMPCS displayed banded textures after mechanical shearing in LC state;[33] branched polymers were not able to form banded textures regardless of attempts at different temperature and shearing rate.

In the case of random copolymers based on MPCS and CMS (Table S1), the thermotropic behaviors similar to the copolymers of MPCS with styrene or methyl methacrylate were observed. The copolymers with molar fraction of MPCS units higher than 0.72 were able to form LC phase. When more CMS was introduced into PMPCS backbone, the mesophase was completely depressed. In addition, only less perfect banded textures could be observed in certain copolymers after mechanical shearing in their LC states.

1D Wide-Angle X-ray Diffraction. To examine the ordered structures developed in these copolymers further, 1D-WAXD experiments were run on the as-cast samples. In consistent with POM observations, the mesophase structures of branched PMPCSs were found to rely strongly on the length of MPCS segment. Figure 4 illustrates the temperature variable 1D-WAXD patterns of BP-6 in the low 2θ angle region (between 3° and 10°), which were recorded during the first heating and the subsequent cooling steps, respectively. At room temperature, only a scattering halo was observed. At the temperatures above T_g, the intensity of the scattering halo became a little stronger. The scattering halo returned to its original state at room temperature upon subsequent cooling, suggesting the formation of a reversible and less ordered mesophase in the melt. This agreed well with the POM observation of this sample.

Figure 5 shows the temperature variable 1D-WAXD pattern of BP-18 in the low 2θ angle region. At room temperature, similar to BP-6, only a scattering halo was observed. At higher temperatures, the scattering halo became asymmetric and developed into one broad halo and a narrow reflection peak which centered at $2\theta = 5.3°$ (d-spacing of 1.66 nm) and 5.6° (d-spacing of 1.58 nm), respectively. Raising temperature substantially enhanced the intensity of reflection peak until the highest temperature we studied (i.e., 290 °C), and the peak shifted slightly and continuously to lower 2θ angle due to the thermal expansion. The branched PMPCS was quite thermal stable, and the 1% weight loss temperature was higher than 320 °C. Upon being cooled slowly from 290 °C, the intensity of reflection peak decreased with decreasing temperature. However, the narrow reflection peak still existed even when

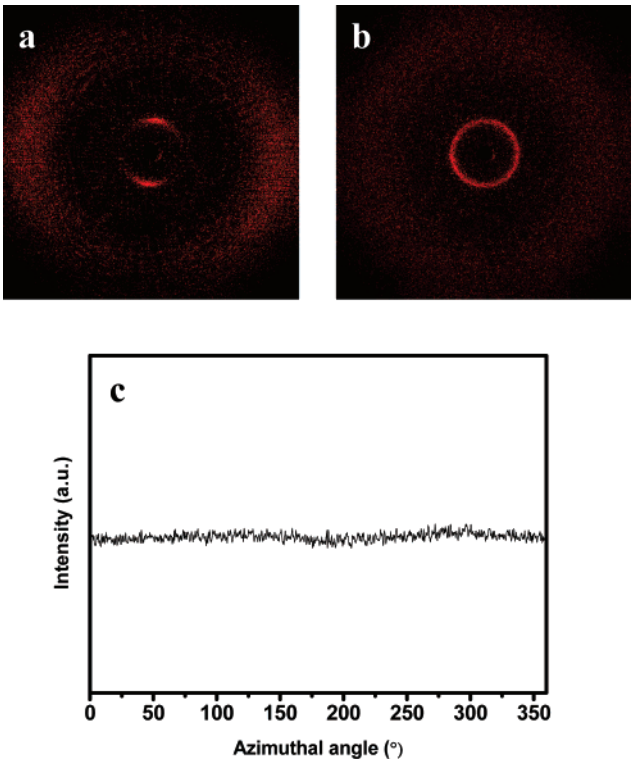

Figure 6. Two-dimensional wide-angle X-ray diffraction fiber patterns of the BP-16. The X-ray incident beam was (a) perpendicular to the fiber axis (the meridian direction), (b) along the meridian direction, and (c) the azimuthal scanning data of the low 2θ angle region diffraction.

the sample was cooled to room temperature, indicating that the mesophase formed at higher temperature could be kept upon cooling although it was less ordered. BP-17 and BP-16 exhibited similar thermal behavior with BP-18 (Figures S5 and S6). The temperature that sharp reflection peaks appeared was 170 °C, and the reflection peaks were centered at $2\theta \approx 5.6°$ (d-spacing of ca. 1.58 nm). Compared with BP-18, the reflection peaks of BP-17 and BP-16 formed at high temperature were much stronger, which implied a more ordered arrangement of polymer chains.

2D Wide-Angle X-ray Diffraction. Figure 6a shows the 2D-WAXD pattern of the oriented BP-16 sample with the X-ray incident beam perpendicular to the orientation direction (equator direction). A pair of strong diffraction arcs were present at $2\theta = 5.60°$ (d spacing of 1.58 nm), implying the ordered structure developed along the direction perpendicular to the fiber axis on the nanometer scale. In the high 2θ angle region, a scattering halo appeared at $2\theta = 20.36°$ (d spacing of 0.43 nm) with a

Scheme 2. Schematic Illustration of Compact and Geometrically Anisotropic Structure of Branched Poly{2,5-bis[(4′-methoxyphenyl)oxycarbonyl]styrene} (PMPCS) To Form a Liquid Crystalline Phase

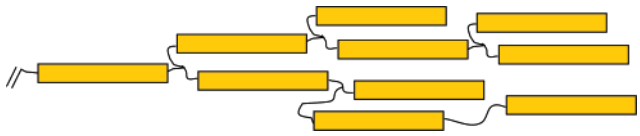

broad azimuthal distribution, which indicated only short-range order existed along the orientation direction. There was no higher order diffraction identified even after a prolonged exposure time except for the pair of strong diffraction arcs displayed in the low 2θ angle region. Figure 6b shows the diffraction patterns of the oriented HBP-16 with the shearing direction parallel to the X-ray incident beam. BP-16 presented a ring pattern centered at $2\theta = 5.60°$ (d spacing of 1.58 nm). Azimuthal scanning gave an isotropic intensity distribution (Figure 6c); thus, the liquid crystalline structure of BP-16 should be Φ_N phase. Other branched polymers displayed 2D-WAXD patterns similar to that of BP-16 and therefore had identical Φ_N phase.

It is interesting to compare the thermotropic properties of linear PMPCS, branched PMPCS, and random copolymers of MPCS and CMS. Linear PMPCS forms Φ_N and Φ_{HN} phases depending on its MW.[33] It is believed that the direct linking makes the interaction between rigid, bulky side groups and polymer backbone so strong that side chains and main chain can act as a whole to achieve mesophase; i.e., the mesogenic units are extended macromolecules themselves. The incorporation of nonmesogenic unit such as styrene and methyl methacrylate would generate constitutional disorder, which dilutes the concentration of mesogenic units and disrupts the interactions between backbone and side groups.[47] As a result, the mesophase is destabilized. For the random copolymers based on MPCS and CMS to form a mesophase, more than 24 mol % CMS can be tolerated. The depressing effect of constitutional irregularity caused by CMS on the LC property of PMPCS is even more pronounced in branched polymers than in random copolymers. For the branched PMPCS to generate a mesophase, the feed molar ratio of MPCS to CMS should not be less than 30 and $M_{n,\,GPC}$ should be higher than 1.21×10^4 Da when [MPCS]/[CMS] in feed equaled to 32, which is also larger than the $M_{n,\,GPC}$ value for linear PMPCS to form a mesophase. This might be rationalized by the mechanism of branched PMPCS to generate a mesophase (Scheme 2). We considered the conformational isomerism rule for the hyperbranched polyethers, polyesters, and dendrimers to achieve mesophases,[6,7,10] which was proposed by Percec and co-workers first, was applicable to branched PMPCS as well. Branched PMPCS distinguished Percec's polymers by the presence of long PMPCS segment between branching points originated from CMS. On the one hand, CMS unit separated PMPCS segment as a structural defect. On the other hand, it acted as flexible points that enabled branched PMPCS to undergo conformation change to take elongated, nonspherical molecular shapes with a greater ease.

Conclusion

Novel branched MJLCPs based on CMS and MPCS were prepared through ATR−SCVCP. At the early stage of copolymerization, CMS acted mainly as an initiator to induce the ATRP of MPCS due to both relatively large molar ratio of MPCS to CMS in feed and much higher reactivity of MPCS than CMS. The branched structure formed with the participation of polymerization of vinyl group of CMS. Thus, obtained copolymers showed depressed thermotropic LC properties compared to linear PMPCS and even the random copolymers of MPCS and CMS synthesized via conventional radical copolymerization. This was consistent with the general rule that dendrimers and hyperbranched polymers disfavor the formation of mesophase since the mesogens on the treelike skeleton are not prone to pack orderedly. To generate a stable mesophase, branched PMPCS should have a minimum MW, and the feed molar ratio of MPCS to CMS should be higher than 30. Although linear PMCPS forms columnar nematic phase (Φ_N) and hexatic columnar nematic phase (Φ_{HN}) depending on MW, the branched polymers showed just a Φ_N phase.

Acknowledgment. The financial support from the National Natural Science Foundation of China (Grants 20674001 and 20134010) and the National Distinguished Young Scholar Fund (Grant 20325415) is gratefully acknowledged.

Supporting Information Available: Estimation of r_{MPCS} and r_{CMS}, GPC curves of the branched polymers, DSC traces of BP-2−BP-12, and one-dimensional wide-angle X-ray diffraction patterns of BP-16 and -17. This information is available free of charge via the Internet at http://pubs.acs.org.

References and Notes

(1) George, R. N.; Charles, N. M. *Angew. Chem., Int. Ed.* **1991**, *30*, 1176−1178.
(2) Brigitte, V. *Acta Polym.* **1995**, *46*, 87−99.
(3) George, R. N.; Enfei, H.; Charles, N. M. *Chem. Rev.* **1999**, *99*, 1689−1746.
(4) Fréchet, J. M. J. *Science* **1994**, *263*, 1710−1715.
(5) Kim, Y. H. *J. Am. Chem. Soc.* **1992**, *114*, 4947−4948.
(6) Percec, V.; Cho, C. G.; Pugh, C.; Tomazos, D. *Macromolecules* **1992**, *25*, 1164−1176.
(7) Percec, V.; Kawasumi, M. *Macromolecules* **1992**, *25*, 3843−3850.
(8) Percec, V.; Chu, P.; Kawasumi, M. *Macromolecules* **1994**, *27*, 4441−4453.
(9) Percec, V.; Chu, P.; Ungar, G. *J. Am. Chem. Soc.* **1995**, *117*, 11441−11454.
(10) Hahn, S. W.; Yun, Y. K.; Jin, J. I.; Han, O. H. *Macromolecules* **1998**, *31*, 6417−6425.
(11) Choi, S. H.; Lee, N. H.; Cha, S. W.; Jin, J. I. *Macromolecules* **2001**, *34*, 2138−2147.
(12) Kricheldorf, H. R. *Pure Appl. Chem.* **1998**, *70*, 1235−1238.
(13) Reina, A.; Gerken, A.; Zemann, U.; Kricheldorf, H. R. *Macromol. Chem. Phys.* **1999**, *200*, 1784−1791.
(14) Bauer, S.; Ringsdorf, H.; Fischer, H. *Angew. Chem., Int. Ed.* **1993**, *32*, 1589−1592.
(15) Sunder, A.; Quincy, M.; Mülhaupt, R.; Frey, H. *Angew. Chem., Int. Ed.* **1999**, *38*, 2928−2930.
(16) Chen, Y.; Shen, Z.; Gehringer, L.; Frey, H.; Stiriba, S. E. *Macromol. Rapid Commun.* **2006**, *27*, 69−75.
(17) Zhang, X.; Chen, Y. M.; Gong, A. J.; Chen, C. F.; Xi, F. *Liq. Cryst.* **1998**, *25*, 767−769.
(18) He, X. H.; Yan, D. Y.; Mai, Y. Y. *Eur. Polym. J.* **2004**, *40*, 1759−1765.
(19) Ganicz, T.; Pakula, T.; Fortuniak, W. *Polymer* **2005**, *46*, 11380−11388.
(20) He, X. H.; Yan, D. Y. *Macromol. Rapid Commun.* **2004**, *25*, 949−953.
(21) Fréchet, J. M. J.; Henmi, M.; Gitsov, I.; Aoshima, S.; Leduc, M. R.; Grubbs, R. B. *Science* **1995**, *269*, 1080−1083.
(22) Hawker, C. J.; Fréchet, J. M. J.; Grubbs, R. B.; Dao, J. *J. Am. Chem. Soc.* **1995**, *117*, 10763−10764.
(23) Zhou, Q. F.; Li, H. M.; Feng, X. D. *Macromolecules* **1987**, *20*, 233−234.
(24) Zhou, Q. F.; Li, Z. X.; Wen, Z. Q. *Macromolecules* **1989**, *22*, 491−493.
(25) Zhang, D.; Zhou, Q. F.; Ma, Y. G.; Wan, X. H.; Feng, X. D. *Polym. Adv. Technol.* **1997**, *8*, 227−233.
(26) Wan, X. H.; Zhou, Q. F.; Zhang, D.; Zhang, Y.; Feng, X. D. *Chem. J. Chin. Univ.* **1998**, *19*, 1507−1512.
(27) Wan, X. H.; Zhang, F.; Wu, P.; Zhang, D.; Feng, X. D.; Zhou, Q. F. *Macromol. Symp.* **1995**, *96*, 207−218.
(28) Zhi, J. G.; Liu, A. H.; Zhu, Z. G.; Lü, X. C.; Fan, X. H.; Chen, X. F.; Wan, X. H.; Zhou, Q. F. *Acta Polym. Sin.* **2005**, *5*, 774−778.

(29) Xu, G. Z.; Wu, W.; Shen, D. Y.; Hou, J. N.; Zhang, S. F.; Xu, M.; Zhou, Q. F. *Polymer* **1993**, *34*, 1818−1822.
(30) Zhou, Q. F.; Wan, X. H.; Zhu, X. L.; Zhang, F.; Feng, X. D. *Mol. Cryst. Liq. Cryst.* **1993**, *231*, 107−117.
(31) Wan, X. H.; Tu, Y. F.; Zhang, D.; Zhou, Q. F. *Polym. Int.* **2000**, *49*, 243−247.
(32) Zhang, D.; Liu, Y. X.; Wan X. H.; Zhou, Q. F. *Macromolecules* **1999**, *32*, 5183−5185.
(33) Ye, C.; Zhang, H. L.; Huang, Y.; Chen, E. Q.; Lu, Y. L.; Shen, D. Y.; Wan, X. H.; Shen, Z. H.; Cheng, S. Z. D.; Zhou, Q. F. *Macromolecules* **2004**, *37*, 7188−7196.
(34) Tu, Y. F.; Wan, X. H.; Zhang, D.; Zhou, Q. F. *J. Am. Chem. Soc.* **2000**, *122*, 10201−10205.
(35) Tenneti, K. K.; Chen, X. F.; Li, C. Y.; Tu, Y. F.; Wan, X. H.; Zhou, Q. F.; Sics, I.; Hsiao, B. S. *J. Am. Chem. Soc.* **2005**, *127*, 15481−15490.
(36) Yi, Y.; Fan, X. H.; Wan, X. H.; Li, L.; Zhao, N.; Chen, X. F. *Macromolecules* **2004**, *37*, 7610−7618.
(37) Tu, Y. F.; Wan, X. H.; Zhang, H. L. *Macromolecules* **2003**, *36*, 6565−6569.
(38) Pan, Q. W.; Gao, L. C.; Chen, X. F.; Fan, X. H.; Zhou, Q. F. *Macromolecules* **2007**, *40*, 4887−4894.
(39) Matyjaszewski, K.; Nanda, A. K. *Macromolecules* **2005**, *38*, 2015−2018.
(40) Wermer, M. W.; Frechet, J. M. J. *J. Polym. Sci., Part A: Polym. Chem* **1998**, *36*, 955−970.
(41) Brereton, M. G. *Macromolecules* **1990**, *23*, 1119−1131.
(42) Kelen, T.; Tüdos, F. *J. Macromol. Sci., Chem.* **1975**, *A9*, 1−27.
(43) Zhao, Y. F.; Yi, Y.; Fan, X. H.; Chen, X. F.; Wan, X. H.; Zhou, Q. F. *J. Polym. Sci., Part A: Polym. Chem.* **2005**, *43*, 2666−2674.
(44) Gopalan, P.; Ober, C. K. *Macromolecules* **2001**, *34*, 5120−5124.
(45) Markoski, L. J.; Moore, J. S. *Macromolecules* **2001**, *34*, 2695−2701.
(46) Murali, M.; Samui, A. B. *J. Polym. Sci., Part A: Polym. Chem*. **2006**, *44*, 3986−3994.
(47) Liu, A. H.; Zhi J. G.; Cui, J. X.; Wan, X. H.; Zhou, Q. F. *Macromolecules* **2007**, *40*, 8233−8243.

MA7024368